

## The Electronic Origin of the Dual Fluorescence in Donor–Acceptor Substituted Benzene Derivatives

Semyon Cogan, Shmuel Zilberg,\* and Yehuda Haas\*

Contribution from the Department of Physical Chemistry and the Farkas Center for Light Induced Processes, The Hebrew University of Jerusalem, Jerusalem, Israel

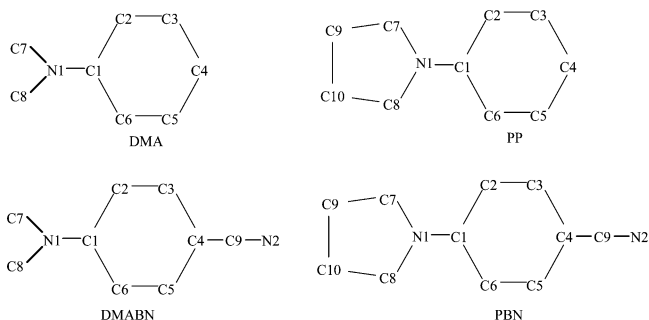
Received July 21, 2005; E-mail: yehuda@chem.ch.huji.ac.il

**Abstract:** The origin of the dual fluorescence of DMABN (dimethylaminobenzonitrile) and other benzene derivatives is explained by a charge transfer model based on the properties of the benzene anion radical. It is shown that, in general, three low-lying electronically excited states are expected for these molecules, two of which are of charge transfer (CT) character, whereas the third is a locally excited (LE) state. Dual fluorescence may arise from any two of these states, as each has a different geometry at which it attains a minimum. The Jahn–Teller induced distortion of the benzene anion radical ground state helps to classify the CT states as having quinoid (Q) and antiquinoid (AQ) forms. The intramolecular charge transfer (ICT) state is formed by the transfer of an electron from a covalently linked donor group to an anti-bonding orbital of the  $\pi$ -electron system of benzene. The change in charge distribution of the molecule in the CT states leads to the most significant geometry change undergone by the molecule which is the distortion of the benzene ring to a Q or AQ structure. As the dipole moment is larger in the perpendicular geometry than in the planar one, this geometry is preferred in polar solvents, supporting the twisted intramolecular charge transfer (TICT) model. However, in many cases the planar conformation of CT excited states is lower in energy than that of the LE state, and dual fluorescence can be observed also from planar structures.

### I. Introduction

The origin of the dual fluorescence (DF) observed first in DMABN (the structures and atom numbering convention for the molecules discussed in this paper are shown in Scheme 1) and later in a large number of aniline derivatives continues to puzzle workers in the field.<sup>1</sup> Several models have been proposed, initially based on chemical intuition and more recently supported by quantum chemical calculations. Apart from early models that have since been discounted, the current accepted consensus is that the red-shifted band observed in polar solvents is due to an intramolecular charge transfer state. Time-resolved experiments<sup>2</sup> indicate that fluorescence arises almost instantaneously from a locally excited state (usually referred to as the B state) which is correlated with the  $1^1B_{2u}$  state of benzene ( $L_b$  in Platt's notation<sup>3</sup>). Local excitation means in this context the transfer of an electron from an occupied  $\pi$  MO to an unoccupied one, both localized primarily in the benzene ring. Red-shifted emission, assigned to a charge transfer state, is also observed, usually after some time delay (in the ps range). In this state an electron was transferred from the donor part of the system (the amino or pyrrolo group) to the acceptor part (the phenyl or cyanophenyl group).<sup>1</sup> The nature of the CT state, in particular its geometry, has been a matter of dispute. It was suggested by some authors<sup>1,4</sup> that the state is correlated with the  $L_a$  state, which is the second locally excited state in the Franck–Condon

**Scheme 1.** Structures and Atom Numbering Convention for Dimethylaniline (DMA), Dimethylaminobenzonitrile (DMABN), *N*-Phenylpyrrole (PP), and *para*-Phenylbenzonitrile (PBN)



region. Two leading models appear to prevail at this time. In the twisted intramolecular charge transfer (TICT) model<sup>5</sup> the emitting species is assumed to have a twisted geometry, with the torsion angle  $\phi$  between the benzene ring and the amino (or pyrrolo) group close to  $90^\circ$ . The planar intramolecular charge transfer (PICT) model<sup>6</sup> proposes a planar structure ( $\phi = 0^\circ$ ) for the emitting state. In this paper the term torsion angle will refer to  $\phi$  unless otherwise stated. Experimental evidence advanced for both models has been largely circumstantial, as direct measurement of the structure of the emitting species turns out to be experimentally difficult.

(1) Grabowski, Z. R.; Rotkiewicz, K.; Rettig, W. *Chem. Rev.* **2003**, *103*, 3899.  
 (2) Leinhos, U.; Kühnle, W.; Zachariasse, K. *J. Phys. Chem. A* **1991**, *95*, 2013.  
 (3) Platt, J. R. *J. Chem. Phys.* **1949**, *17*, 484.  
 (4) Rettig, W.; Wermuth, G.; Lippert, E. *Ber. Bunsen-Ges. Phys. Chem.* **1979**, *83*, 692.

(5) (a) Rotkiewicz, K.; Grellmann, K. H.; Grabowski, Z. R. *Chem. Phys. Lett.* **1973**, *19*, 315. (b) Grabowski, Z. R.; Rotkiewicz, K.; Siemiarczuk, A.; Cowley, D. J.; Baumann, W. *Nouv. J. Chim.* **1979**, *3*, 443.  
 (6) Schuddeboom, W.; Jonker, S. A.; Warman, J. M.; Leinhos, U.; Kühnle, W.; Zachariasse, K. A. *J. Phys. Chem.* **1992**, *96*, 10809.

Nonetheless, equally convincing indirect evidence has been presented for the TICT and PICT models. For instance, by a suitable construction, Dobkowski et al. showed that the CT process is accompanied by syn–anti isomerization around the  $C_{\text{phenyl}}-N$  bond in the photoisomerization of 2-(*N*-methyl-*N*-isopropylamino)-5-cyanopyridine, a process that implies the intermediacy of a perpendicular moiety.<sup>7</sup> On the other hand, Yoshihara et al. showed that a planarized molecule that cannot attain a perpendicular geometry exhibits dual emission.<sup>8</sup> The planar rigidized molecule fluorazene (FPP) was shown to undergo fast reversible intramolecular charge transfer (ICT) in the excited state, similar to that of its flexible counterpart *N*-phenylpyrrole (PP). This result shows that intramolecular charge transfer to a planar ICT state can occur efficiently and thus convincingly demonstrates that large amplitude motions such as those necessary for the formation of a TICT state are not required.

One of the puzzling experimental aspects of most systems is the nature of the temperature dependence of the CT process. Attempts to fit the observed data to an Arrhenius expression lead to rather small activation energies (typical values range between 5 and 15 kJ/mol<sup>1,9</sup>). Some authors propose a non-Arrhenius behavior of the system, suggesting that there is no energy barrier in the usual sense and that the process is controlled by entropy considerations.<sup>10</sup>

In the last 10 years or so, many attempts to elucidate the nature of the excited states using quantum chemical calculations have been made. Gomez et al.<sup>11</sup> who recently summarized competently the current state-of-the-art emphasize the role of conical intersections in the evolution of the system from the initially excited state to the emitting ones. Their analysis which refers to gas-phase systems clearly distinguishes between nonadiabatic radiationless transition between  $S_2$  and  $S_1$  on one hand, and adiabatic equilibration on the emitting  $S_1$  surface on the other. On each potential surface they identify more than one minimum. Liquid solution work refers mostly to processes taking place on the  $S_1$  surface which is rapidly populated even if a higher state is initially excited.<sup>12,13</sup>

Some time ago we offered a model that predicts this situation for the pyrrole derivatives *N*-phenylpyrrole (PP) and pyrrolbenzotrile (PBN).<sup>14</sup> In that paper the primary role of the benzene ring was pointed out—it is not acting merely as a spacer between the donor and the acceptor but is essential for understanding the electronic structure of the excited states. This approach follows the classical work of Kimura and co-workers,<sup>15</sup> who showed that the vacuum UV absorption spectra of aniline and its derivatives include, in addition to the two LE transitions derived from the  $\pi$  electron system of benzene, two bands due to transitions from the donor  $\pi$  orbital to the benzene ring. In

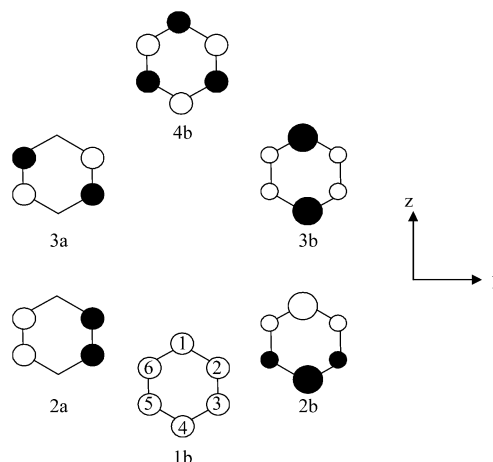


**Figure 1.** The 6  $\pi$  orbitals of benzene labeled as in  $C_2$  symmetry.

ref 14 the TICT and PICT models were identified as being due to CT states in which the benzene ring is distorted to an anti-quinoid (AQ) and quinoid (Q) structures, respectively; the AQ form was found to be twisted, and the Q form planar. Dreyer and Kummrow<sup>16</sup> identified a different CT state in DMABN, in which the benzene ring assumes a quinoid structure, whereas the dimethyl amino group is  $90^\circ$  twisted with respect to the ring ( $\phi = 90^\circ$ ). This species, whose structure was confirmed by later workers,<sup>11,17</sup> did not fit with our early model. We were therefore motivated to consider further options for the CT state by taking into account the structure of the acceptor regarded as a derivative of the benzene anion radical. It turns out that a model based on the idea that the benzene ring is the principal electron acceptor leads naturally to the four distinct lowest-lying electronic excited states in these systems:<sup>15</sup> two are principally of LE nature, whereas the other two are CT-types.

The model readily accounts for the observed dual emission in both amino and pyrrole derivatives (while also pointing out the differences between these two groups) and also appears to resolve the TICT/PICT debate. It is shown that both planar and twisted forms of the molecule in the CT state may be fluorescent, depending on the structure of the system and on environmental parameters such as the solvent. Supplementary to the previous model based on the electronic properties of the neutral molecule, in which only the planar Q-form was considered, the present model predicts also the existence of a perpendicular Q-form having a large dipole moment. A comparison between the two models is outlined in section VI.d.

## II. Model

We begin by recalling the standard MO description of the electronically excited states of benzene. As most experimental data on DF systems relate to para-disubstituted benzene derivatives,  $C_2$  symmetry is used in the presentation. This simplification can be easily removed for any required specific system.

The six  $\pi$ -orbitals of benzene are sketched in Figure 1 which also shows the coordinate system used (the  $z$ -axis is taken along the long axis of the hexagon).

- (7) Dobkowski, J.; Wojcik, J.; Kozminski, W.; Kols, R.; Waluk, J.; Michl, J. *J. Am. Chem. Soc.* **2002**, *124*, 2406.  
 (8) Yoshihara, T.; Druzhinin, S. I.; Zachariasse, K. A. *J. Am. Chem. Soc.* **2004**, *126*, 8535.  
 (9) Il'ichev, Y. V.; Kühnle, W.; Zachariasse, K. A. *J. Phys. Chem. A* **1998**, *102*, 5670.  
 (10) Rettig, W. *Ber. Bunsen-Ges. Phys. Chem.* **1991**, *95*, 259.  
 (11) Gomez, I.; Reguero, M.; Boggio-Pasqua, M.; Robb, M. A. *J. Am. Chem. Soc.* **2005**, *127*, 7119.  
 (12) Dahl, K.; Biswas, R.; Ito, N.; Maroncelli, M. *J. Phys. Chem. B* **2005**, *109*, 1563.  
 (13) Yoshihara, T.; Galiewsky, V. A.; Druzhinin, S. I.; Saha, S.; Zachariasse, K. A. *Photochem. Photobiol. Sci.* **2003**, *2*, 342.  
 (14) Zilberg, S.; Haas, Y. *J. Phys. Chem. A* **2002**, *106*, 1.  
 (15) Kimura, K.; Tsubomura, H.; Nagakura, S. *Bull. Chem. Soc. Jpn.* **1964**, *37*, 1336.

- (16) Dreyer, J.; Kummrow, A. *J. Am. Chem. Soc.* **2000**, *122*, 2577.  
 (17) Köhn, A.; Hättig, C. *J. Am. Chem. Soc.* **2004**, *126*, 7399.

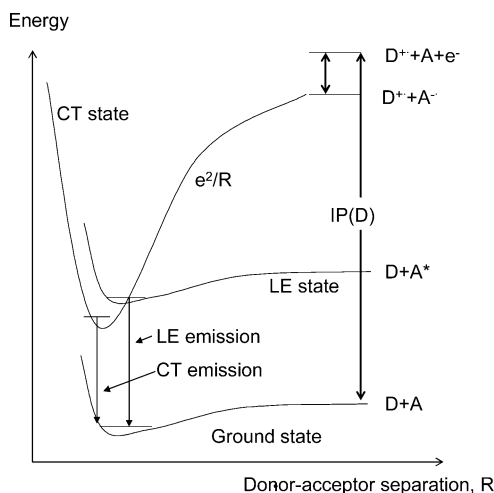


**Figure 2.** Schematic presentation of the energy level diagram of a system having dual fluorescence due to a CT state.

The orbitals are labeled as a- or b-type, as is appropriate for this symmetry group. The lowest-lying configurations may be written as follows:

$$\text{ground state } (1^1A) = (1b)^2(2b)^2(2a)^2 \quad (1)$$

$$\text{LE state 1 } (1^1B) = (1b)^2(2b)^2(2a)^1(3b)^1 - (1b)^2(2b)^1(2a)^2(3a)^1 \quad (2)$$

$$\text{LE state 2 } (2^1A) = (1b)^2(2b)^2(2a)^1(3a)^1 + (1b)^2(2b)^1(2a)^2(3b)^1 \quad (3)$$

In  $D_{6h}$  benzene the two low-lying excited states are  $1^1B_{2u}$  and  $1^1B_{1u}$  respectively. It is well-known that the  $1^1B_{2u}$  state is a purely covalent one (an anti-combination of the two Kekulé structures), whereas the  $1^1B_{1u}$  state is largely ionic (constructed by combining the polar (zwitterionic) VB structures of benzene).<sup>18</sup>

The new feature that we introduce to assign the fluorescence emitted by a CT state is an electronic state that is formed by transferring an electron from an external donor to the benzene ring. The standard model for a CT state following Mulliken's approach<sup>19</sup> is depicted in Figure 2. For a more extended discussion of gas-phase CT systems, see ref 20.<sup>20</sup> In its simplest form the interaction between the acceptor and donor is purely electrostatic ("through space"). The energy of the CT state above the ground state is given approximately by eq 4:

$$\Delta E = IP(D) - EA(A) - e^2/R \quad (4)$$

where  $e$  is the charge transferred and  $R$  the donor-acceptor distance.<sup>21</sup>

In the special case of substituted benzene molecules the benzene ring is the acceptor (as for instance in the case of DMA and PP) and a substituent is the donor. In MO language, the

extra electron may be placed in one of the two degenerate  $\pi^*$  orbitals 3a or 3b ( $e_{2u}$  in  $D_{6h}$ ). The basic model was discussed by Murrell<sup>22</sup> and used by Kimura et al.<sup>15</sup> for aniline and its derivatives. They showed that two CT states are expected, having a and b symmetries in the  $C_2$  symmetry group. An important factor, not explicitly discussed in refs 15 and 22 is the fact that the benzene anion radical, the prototype of all derivatives, undergoes Jahn-Teller (JT) distortion. The Jahn-Teller effect<sup>23</sup> requires that the benzene anion radical will have two different electronic structures which, in principle, have minima at different nuclear geometries. A similar distortion is expected in the intramolecular charge transfer case, even though the molecule is not strictly a high-symmetry Jahn-Teller system. The term pseudo-JT effect has been used for such cases.<sup>24</sup>

Inspection of Figure 1 shows that placing the extra electron in orbital 3a of benzene results in a node between the central carbon atoms 2 and 3 (and also between 5 and 6) leading to an antiquinoid (AQ) structure. If the 3b orbital is populated, a quinoid (Q) structure results in which the C2C3 and C5C6 bond lengths are shortened.<sup>25,26</sup> In the symmetric case (e.g.,  $C_6H_6^{\bullet-}$ ) the potential surface has the shape of a nearly perfect Mexican hat. The molecular frame is distorted to a nearly  $D_{2h}$  symmetry. A DFT calculation<sup>27</sup> shows that there may be a very shallow minimum at a  $C_{2v}$  symmetry, but for all practical purposes the system can oscillate between the Q and AQ forms essentially freely. Optical and ESR experiments indicate an almost equal energy for the two JT distorted structures.<sup>28</sup>

In a donor-substituted anion radical benzene molecule, the donor orbitals are p or  $\pi$  orbitals that have b-type symmetry (for an amino substituent) in the  $C_2$  symmetry group. The donor group, which has a relatively high-lying HOMO (low ionization potential) can by symmetry only interact with the benzene 3b MO. The resulting pair of orbitals (Figure 3) shifts the donor's orbital downward a little, and the benzene's 3b LUMO shifts up, leaving the 3a MO as the LUMO of the substituted system. Addition of an electron to this system to form the anion radical results in a low-energy configuration in which the extra electron is in the 3a MO which becomes the SOMO. According to this model the ground-state configuration of the anion radical is  $2^1A$ , with an AQ structure. (The antiquinoid structure is due to the form of the 3a orbital.) A slightly higher-energy anion radical would be formed if the electron were to be placed in the 3b-D(b) orbital, forming a quinoid structure with a  $2^1B$  symmetry. We note that at the optimal quinoid nuclear geometry the  $2^1B$  state is expected to be lower in energy than the  $2^1A$  state, meaning that the two states cross at certain geometry near the perfect hexagonal one. This conical intersection is directly related to the Jahn-Teller degeneracy at the perfect hexagonal symmetry of the benzene anion radical.

- (18) DaSilva, E. C.; Gerratt, J.; Cooper, D. L.; Raimondi, M. *J. Chem. Phys.* **1994**, *101*, 3866.  
 (19) (a) Mulliken, R. S. *J. Am. Chem. Soc.* **1952**, *74*, 811. (b) Murrell, J. N. *J. Am. Chem. Soc.* **1959**, *81*, 5037.  
 (20) (a) Haas, Y.; Anner, O. In *Photoinduced Electron Transfer*, Part A; Fox, A. M., Chanon, M., Eds.; Elsevier: Amsterdam, 1988; p 305. (b) Haas, Y. In *Electron transfer in Chemistry*; Balzani, V., Ed.; Wiley-VCH: Weinheim, 2001; Vol. 4, p 742.  
 (21) This model has been mentioned in the context of the DF problem of DMABN but has not been fully developed: Rettig, W. *J. Lumin.* **1981**, *26*, 21.

- (22) Murrell, J. N., *Proc. Phys. Soc. (London)* **1955**, *A68*, 969.  
 (23) Jahn, H. A.; Teller, E. *Proc. Roy. Soc. (London)*, **1937**, *A161*, 220.  
 (24) (a) Hobey, W. D. *J. Chem. Phys.* **1965**, *43*, 2187. (b) Jordan, K. D.; Burrow, P. D. *Acc. Chem. Res.* **1978**, *11*, 341.  
 (25) Liehr, A. D. *J. Phys. Chem.* **1963**, *67*, 389.  
 (26) Hinde, A. L.; Poppinger, D.; Radom, L. *J. Am. Chem. Soc.* **1978**, *100*, 4681.  
 (27) Hrovat, D. A.; Hammons, J. H.; Stevenson, C. D.; Borden, W. T. *J. Am. Chem. Soc.* **1997**, *119*, 9523.  
 (28) Optical: (a) Gardner, C. L. *J. Chem. Phys.* **1966**, *45*, 572. (b) Moore, J. C.; Thornton, C.; Collier, W. B.; Devlin, J. P. *J. Phys. Chem.* **1981**, *85*, 350. ESR: (c) Tuttle, T. R.; Weissman, S. I. *J. Am. Chem. Soc.* **1958**, *80*, 5342. (d) Lawler, R. G.; Bolton, J. R.; Fraenkel, G. K.; Brown, T. H. *J. Am. Chem. Soc.* **1964**, *86*, 520.

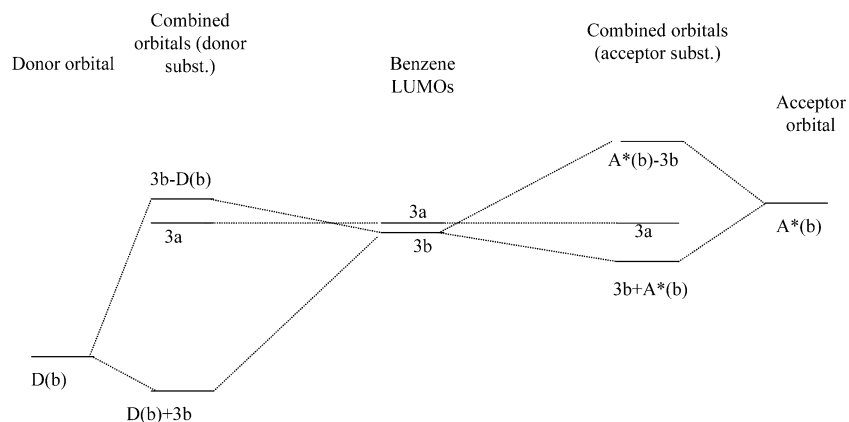


**Figure 3.** MO correlation diagram showing the electronic structure of donor and acceptor substituted benzene. D(b) is a donor bonding or nonbonding orbital and A\*(b) is an antibonding acceptor orbital, both b-type. 3a and 3b are the two lowest unoccupied MOs of benzene.

An efficient electron *acceptor* group has a relatively low-lying anti-bonding orbital available for insertion of an electron. In the case of the cyano moiety, this orbital, which lies slightly above the 3a and 3b orbitals, can only interact with the 3b orbital pushing it down so that the LUMO of the system is now primarily 3b+A\*(b), becoming the SOMO upon adding an electron. The expected ground-state configuration in this case is  ${}^2B$ , and the preferred molecular symmetry, quinoidal. The second electronic state (an electronically excited state) is a  ${}^2A$  one, formed by adding the electron to the somewhat higher-lying 3a MO (cf. Figure 3).

When both a donor and acceptor are substituted onto the benzene ring, the relative energies of the first two electronic states of the anion radical depend on the nature of the substituents. As in the case of the benzene anion radical, two stationary points (having Q and an AQ structures) of similar energies are expected.<sup>29</sup> In the substituted molecules, the energy differences are larger than in the parent anion radical, but still rather small, of the order of 1–10 kcal/mol.<sup>29</sup>

The case of neutral CT electronically excited states is analogous to that of the anion radical, except that in this case the electron added onto the benzene ring comes from a donor that is covalently linked to it. The resulting system carries no net electric charge, but as in the anion radical, two electronic states are expected from the model, both having CT character. Since the ionization potential of donors is much larger than the electron affinity of the acceptors in all cases, these two states are normally expected to be electronically excited states, in addition to the two locally excited (LE) states ( $L_b$  and  $L_a$ ). The two charge transfer states will be labeled as the CT(Q) and CT-(AQ) forms for the quinoid and antiquinoid structures, respectively. *In distinction with the previous paper, here we do not identify the CT(Q) state with the PICT model, nor the CT(AQ) one with the TICT. The Q, AQ nomenclature refers strictly to the electronic structure of the benzene ring, distorted from perfect  $D_{6h}$  symmetry. In principle, each structure may appear with any torsion angle between the benzene and the amino (pyrrolo) group.* The LE states are located at about 4.5–5.5 eV above the ground state. A simple calculation based on the energy scheme of Figure 2 and eq 4 shows that for the CT states to be at about the same energy and assuming a full electron transfer from a substituent to the ring (separation between the

centers of the negative and positive charges about 3–4 Å), the term  $IP(D) - EA(A)$  must be in the range of 9–11 eV. The electron affinity of benzene in the gas phase is estimated at –1.1 eV,<sup>24</sup> that of cyanobenzene at –0.57.<sup>30</sup> Therefore, the donors should have an ionization potential of 8–10 eV for the LE and CT levels to be close lying.

In the simple MO picture, the properties of the CT states depend on the nature of the donating orbital. Consider first the case of PP and PBN (the case of DMA and other aniline derivatives is different, as discussed below). It turns out (see section IV.c) that the HOMO is centered on the butadiene fragment (Scheme 2) and has a node at the nitrogen atom. In this case the interaction between the donor and acceptor orbitals is very small, and the system can be viewed to a very good approximation as having two types of electronic states. As in the case of benzene, the LE states are due to transitions from the benzene HOMOs to the benzene LUMOs, Scheme 2. In addition, two CT states of similar energies but different symmetries arise from the transfer of an electron from the HOMO of the pyrrole group to the two nearly degenerate benzene LUMOs 3a and 3b. Since there is a node at the nitrogen atom, torsion around the  $C_{\text{phenyl}}-N_{\text{amine}}$  bond is not expected to affect the energies of the transitions.<sup>31</sup>

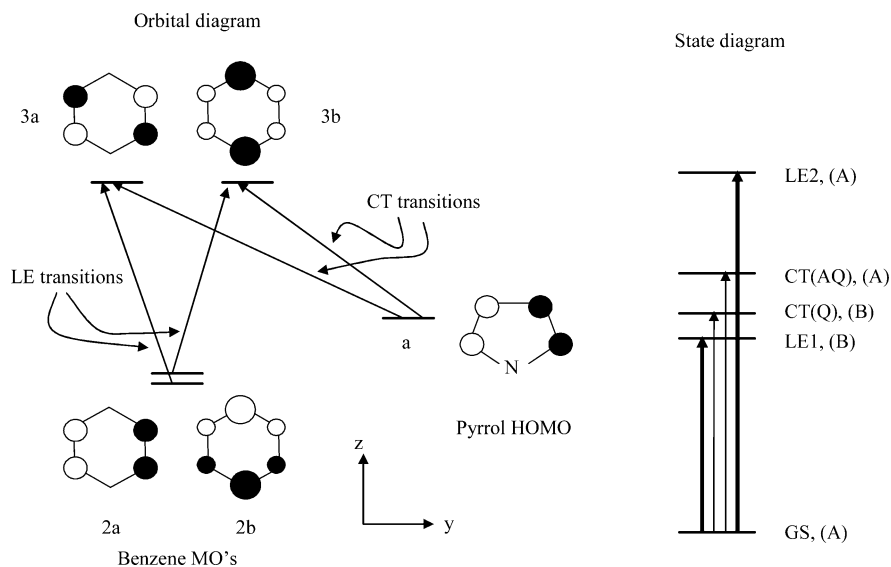
In the aniline derivatives the HOMO is the lone pair orbital of the N-atom. Using again the single configuration approximation, at the perpendicular geometry it does not interact with the  $\pi$ -electron system of the aromatic ring, and complete electron transfer can occur (similar to the pyrrole case). For torsional angles different from 90°, interaction between the two  $\pi$ -electron systems may become nonzero if they have the same symmetry. *The interaction is related to the overlap between the N atom and the benzene MOs and thus increases as the twist angle approaches zero (planar form).* The CT state is therefore most efficiently formed at the perpendicular geometry, at which the interaction is minimal. This is the physical origin of the TICT model proposed by the Grabowski et al.<sup>5</sup>

In the pyrrole derivatives, the lone pair orbital of the nitrogen atom lies at a somewhat lower energy than the butadiene-centered orbital (about 0.3 eV, see below). Transfer of an

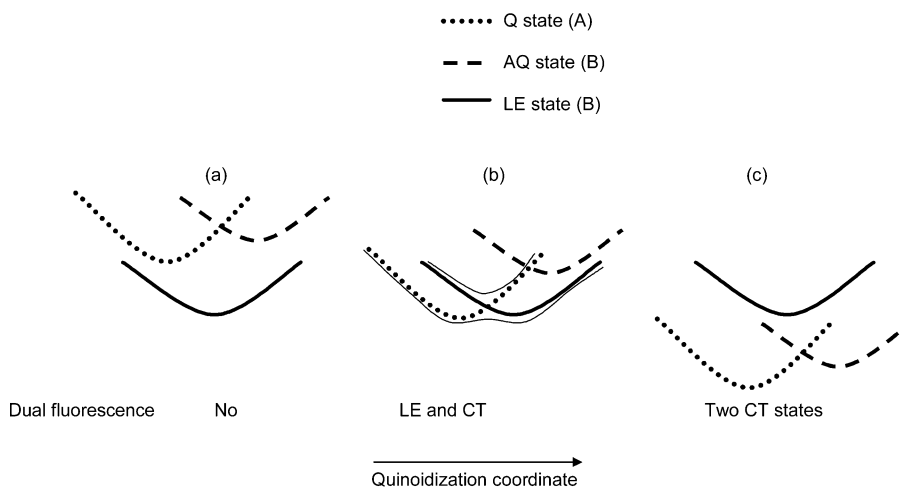
(29) Beregovaya, I. V.; Shchegoleva, L. N. *Int J. Quantum Chem.* **2002**, *88*, 481.

(30) Burrow, P. D.; Howard, A. E.; Johnston, A. R.; J. A.; Jordan, K. D. *J. Phys. Chem.* **1992**, *96*, 7570, 350.

(31) These qualitative single MO based comments refer to the leading configuration in the CI-MO analysis of the molecules. All computations were carried out using a very large number of configurations. A VB analysis of the data leads to similar conclusions.

**Scheme 2.** Schematic Presentation Showing the Frontier Orbitals of Benzene and Pyrrole and the Origin of the LE and CT Transitions in *N*-Phenylpyrrole<sup>a</sup>

<sup>a</sup> Left: MO diagram; right: state diagram and optical transitions from the ground state (GS). The line thickness schematically represents the oscillator strengths.<sup>32</sup> The A and B labels refer to the irreducible representations in the  $C_2$  symmetry group. The states LE1 and LE2 correspond to the  $L_b$  and  $L_a$  states in Platt's notation, respectively. They are referred to below as the LE and  $L_a$ /CT states, respectively.

**Figure 4.** A schematic energy diagram showing the nature of dual fluorescence from the three-state system proposed by the model. Only the lower-lying LE state is shown.

electron from this orbital to the two benzene 3a and 3b orbitals is expected to create two additional CT states, lying at a somewhat higher energy than the two discussed above. Thus, the pyrrole derivatives are expected to have four CT states, whereas the aniline derivatives only two. The two higher-lying states of the pyrrole family are of the same nature as the two CT states of the aniline group.

Figure 4 shows schematically the energy levels of the three lowest-lying excited states of pyrrole or aniline derivatives (one LE and the two CT states) along the symmetric coordinate  $Q_{\text{Quin}}$  that connects the Q and AQ forms through the conical intersection for three typical cases. It is assumed in this case that the LE and Q states are of B-type symmetry, and the AQ one is A-type (as is the case for the aniline derivatives, see Table 1 below). In Figure 4a the LE state is much lower in energy than the two CT ones so that no DF is expected. In 4b all three levels are close to each other. As the Q state and the LE one have the same symmetry, their interaction may lead to a double minimum on the  $S_1$  potential surface. In 4c both CT

states are lower than the LE state. Dual fluorescence is possible from the two CT states. Whatever the case may be, a system exhibiting DF has at least one  $S_1/S_2$  conical intersection.<sup>14,11</sup>

In our previous communication the planar quinoid (Q) and the perpendicular antiquinoid (AQ) forms of the CT were introduced. The electronic structure of the planar Q form due to an electron transfer from the nitrogen lone pair correlates with the second LE state, referred to in this paper as the  $L_a$ /CT state. The perpendicular Q form was not discussed in ref 14.

### III. Computational Details

CASSCF calculations were performed using the GAMESS<sup>33</sup> electronic structure program, or the GAUSSIAN suite of programs.<sup>34</sup> The active space for all molecules included all  $\pi$  orbitals (occupied and unoccupied) including the lone pair of the nitrogen atom. The basis

(32) Proppe, B.; Merchan, M.; Serrano-Andres, L. *J. Phys. Chem. A* **2000**, *104*, 1608.

(33) Schmidt, M. W.; et al. *J. Comput. Chem.* **1993**, *14*, 1347.

(34) Frisch, M. A.; et al. *Gaussian 98*, revision A.9; Gaussian, Inc.: Pittsburgh, PA, 1998.

**Table 1.** Calculated Energies (first row) and Dipole Moments (D)<sup>a</sup> (second row) of the First Five Electronic States for All Molecules at Their Optimized Geometries<sup>b</sup>

molecule	DMA	DMABN	PP	PBN
GS	−363.75218 1.6	−405.50893 6.5	−438.33075 −1.9	−530.07822 3.5
LE	4.57 (1B) 2.3	5.14 (1B) 7.0	5.41 (1B) 0.1	5.46 (1B) 2.8
CT(Q)	5.09 (1A) 7.7	4.79 (1A) 15.3	5.78 (1B) 10.3	5.34 (1B) 17.6
CT(AQ)	5.29 (1B) 9.8	5.16 (1B) 14.8	5.70 (2A) 11.0	5.39 (2A) 16.1
L <sub>a</sub> /CT(Q)	6.37 8.2	6.02 (2A) 13.7	5.74(2A) −0.7	6.07 (2A) 10.6
CT(Q') <sup>c</sup>			6.22 (3A) 10.0	<i>e</i>
CT(AQ') <sup>c</sup>			6.26(2B) 11.1	<i>e</i>
S <sub>1</sub> (exp) <sup>d</sup>	4.08	4.00	4.40	4.29

<sup>a</sup> Positive dipole moments indicate negative charge on the phenyl part. <sup>b</sup> The symmetries (in parentheses, C<sub>2</sub> group) are also shown. Ground-state energies are in hartree units, other states in eV relative to GS. For PP two higher-lying states are also listed, see text. The experimental energy of the S<sub>1</sub> state as measured in a supersonic jet is also listed for comparison. DMA: CASSCF(8,7)/DZV; DMABN: CASSCF(12,10)/DZV; PP: CASSCF(12,10)/DZV; PBN: CASSCF(12,11)/DZV. <sup>c</sup> The notation CT(Q') and CT(AQ') is used to designate the second quinoid and antiquinoid CT states arising from the transfer of an electron from the lone pair nitrogen orbital of PP and PBN. Their electronic nature is similar to that of the CT(Q) and CT(AQ) states of DMABN. <sup>d</sup> References for the experimental values: DMA - 36; DMABN - 37; PP - 38, 39; PBN - 38. <sup>e</sup> The active space used for PBN was estimated to be too small for calculating these electronic states.

set was DZV.<sup>35</sup> The number of electrons used was 8 for DMA and 12 for DMABN, PP, and PBN. In the case of PBN, the two lowest-energy  $\pi$  orbitals were included in the core. In addition some TD-DFT calculations (B3LYP/cc-pVDZ) were also carried out for comparison. Energy optimization was carried out for each species in the standard method, until the first derivative ( $\partial E/\partial Q$ ) vanished for all Cartesian coordinates  $Q$ .

All data reported in this paper were calculated using this large configuration interaction method. In some figures we illustrate the physical nature of the systems using a frontier orbital model, using the configurations that contributed most to the result. However, all states must be understood to include the contributions from all configurations formed by the active space.

#### IV. Numerical Results

The proposed model predicts that, in general, two out of the three low-lying excited electronic states could, in principle, be responsible for the dual emission in these systems. The nature of the emitting states is determined by a delicate balance of several factors: the electron-donating tendency of the donor, the electron-drawing power of the acceptor, and the energy of the LE state. An important prediction of the model is that the potential surface of the CT state is shallow along the quinoidization coordinate, as well as along the torsion one.

**IV.a. Energies of DMA, DMABN, PP, and PBN in Various States.** The energies of the low-lying electronic states of DMA, DMABN, PP, and PBN were calculated at the CASSCF level using C<sub>2</sub> symmetry (no restriction on the torsion angle). Table 1 lists the calculated energies at the different stationary points on the CT and LE states obtained at the CASSCF level, each individually optimized. In DMA and PP the LE state has the

lowest energy, whereas in DMABN and PBN one of the CT states is lowest. In DMA the LE state is lower in energy than the CT states by more than 0.5 eV, in qualitative agreement with the absence of dual fluorescence in this molecule, whereas DF is observed for all others in polar solvents. The energy difference between the CT(Q) states of DMA and DMABN is 0.42 eV, and between PP and PBN −0.44 eV. These differences are fairly close to the difference between the electron affinities of benzene and benzonitrile (0.53 eV), in reasonable agreement with the electrostatic model. In the case of the CT(AQ) state the corresponding calculated differences are smaller (0.25 and 0.31 eV for the DMA/DMABN and PP/PBN pairs, respectively), but also in the expected direction. The L<sub>a</sub>/CT state is found to be planar and lies at a higher energy than the CT(Q) and CT(AQ) states for all molecules except in the case of PP. It also has a smaller dipole moment, as expected when the LE and CT states are mixed. For PP and PBN two further CT(Q) and CT(AQ) structures are found, at about 0.5 eV above their lower-lying counterparts due to electron transfer from the nitrogen lone pair, and their electronic structures are similar to those of the corresponding states of the aniline derivatives. Their dipole moments at the perpendicular structure (about 10 D for PP and 15 D for PBN) are also similar to those of DMA and DMABN, respectively, in their CT states. These structures are labeled by adding a prime, to denote that they are lying at a higher energy than the emitting CT(Q) and CT(AQ) states. They are termed CT(Q') and CT(AQ') in Table 1. Three structures having A-type symmetry (the L<sub>a</sub>/CT, CT(AQ), and CT(Q')) of the pyrrole derivatives are stationary energy points on the S<sub>1</sub> and S<sub>2</sub> potential surfaces. The first two lie on the 2A potential surface, the third on the next higher one 3A. An analogous situation holds for the three B-type structures (LE, CT(Q), and CT(AQ'))—the first two are on the 1B surface, the third on 2B. The experimentally determined energy of the first excited state (gas, phase, jet cooling) is also given in Table 1. Further comparison with experiment is discussed in section V.

The oscillator strengths ( $f$ ) of electric dipole transitions were calculated for all molecules. Numerical values are given in the Supporting Information (Table S1). It was found that the most intense transition in absorption (Franck–Condon region) is to the L<sub>a</sub>/CT(state ( $f$  of the order of 0.2–0.5). The transitions to the LE(B) states were much weaker ( $f \approx 0.01$ ). For transition to the CT(AQ) states, the calculated oscillator strengths were of intermediate value. It is concluded that the strong absorption band observed for these compounds is due to the 1A→2A(L<sub>a</sub>/CT) transition.

The dipole moment at the optimized structures was found to be large for both the CT(Q) and CT(AQ) forms. A rough estimate of the propensity to transfer the electronic charge may be obtained by calculating the dipole moment expected for the transfer of unit charge from the donor to the acceptor. Assuming that the acceptor is the benzene ring and the negative charge is located at its center, and that the donor is the nitrogen atom in the case of DMABN and the pyrrole ring for PP and PBN, a complete transfer would yield a dipole of about 13.5 D for these molecules. Inspection of Table 1 shows that the *change* in dipole moment upon exciting the molecules from the ground state to the CT(Q) is (D) 7.1, 10.6, 12.2, and 14.1 for DMA, DMABN, PP, and PBN, respectively. The corresponding changes for the CT(AQ) state are 8.0, 9.9, 12.9, and 12.5. These values indicate

(35) Several exploratory runs were made for DMABN and PP with a larger basis set including polarization functions (cc-pVDZ), see Supporting Information). The results were practically the same as with the smaller basis set.

**Table 2.** Computed Optimized Geometries of the Four Lowest-Lying States of DMA, DMABN, PP, and PBN (Bond Lengths in Å, Torsion Angle in deg); DMA: CASSCF(8/7)DZV; DMABN: CASSCF(12/10)DZV; PP: CASSCF(12/10)DZV; PBN: CASSCF(12/11)DZV

molecule	DMA	DMABN	PP	PBN	molecule	DMA	DMABN	PP	PBN
		GS					CT(Q)		
term	1 <sup>1</sup> A	1 <sup>1</sup> A	1 <sup>1</sup> A	1 <sup>1</sup> A	term	2 <sup>1</sup> A	2 <sup>1</sup> A	1 <sup>1</sup> B <sup>a</sup>	1 <sup>1</sup> B <sup>a</sup>
C1–C2	1.416	1.415	1.403	1.397	C1–C2	1.448	1.433	1.446	1.428
C2–C3	1.403	1.395	1.402	1.395	C2–C3	1.385	1.375	1.374	1.374
C3–C4	1.404	1.396	1.394	1.396	C3–C4	1.436	1.433	1.422	1.438
C1–N1	1.402	1.393	1.424	1.413	C1–N1	1.453	1.453	1.462	1.459
N1–C7	1.458	1.460	1.390	1.397	N1–C7	1.475	1.476	1.361	1.351
C4–C9		1.443	-	1.446	C4–C9		1.422	-	1.421
C9–N2		1.179	-	1.179	C9–N2		1.187	-	1.187
C7–C9			1.381	1.376	C7–C9			1.460	1.452
C9–C10			1.441	1.443	C9–C10			1.374	1.375
φ	0	0	36.8	36.5	φ	90	90	90	90
		LE					CT(AQ)		
term	1 <sup>1</sup> B	1 <sup>1</sup> B	1 <sup>1</sup> B	1 <sup>1</sup> B	Term	2 <sup>1</sup> B	1 <sup>1</sup> B <sup>(a)</sup>	2 <sup>1</sup> A	2 <sup>1</sup> A
C1–C2	1.448	1.444	1.440	1.441	C1–C2	1.397	1.397	1.400	1.386
C2–C3	1.443	1.440	1.441	1.440	C2–C3	1.462	1.454	1.456	1.452
C3–C4	1.436	1.440	1.427	1.446	C3–C4	1.407	1.397	1.396	1.396
C1–N1	1.390	1.387	1.395	1.413	C1–N1	1.474	1.473	1.464	1.470
N1–C7	1.463	1.464	1.403	1.385	N1–C7	1.471	1.472	1.361	1.360
C4–C9		1.420	-	1.433	C4–C9		1.453	-	1.455
C9–N2		1.171	-	1.162	C9–N2		1.179	-	1.179
C7–C9			1.375	1.372	C7–C9			1.461	1.460
C9–C10			1.447	1.438	C9–C10			1.371	1.374
φ	0	0	19.4	36.3	φ	90	90	31.3	47.1

<sup>a</sup> The 1B states of DMABN, PP, and PBN have two minima, one is LE-type, the other is the CT-type state, each at its optimized geometry.

that the crude electrostatic model provides a fairly good approximation for the charge-transfer process.

**IV.b. Structures of DMA, DMABN, PP, and PBN in Various States.** According to the model presented in section II, the structure of the LE state is expected to be similar to that of the 1<sup>1</sup>B<sub>2u</sub> state of benzene, as excitation is mainly within the benzene moiety. The structure of the benzene ring in both CT-(Q) and CT(AQ) states is expected to be similar to that of the benzene anion radical. Moreover, the C<sub>phenyl</sub>–N<sub>amino</sub> bond is expected to be lengthened in the two CT states. Table 2 lists the calculated structures of some electronic states of the four molecules in their respective minima and stationary points (constrained to C<sub>2</sub> symmetry). Data for the planar Q state, here termed the L<sub>q</sub>/CT state and the AQ states were reported in ref 14 for PP and PBN.

Inspection of Table 2 reveals that in all molecules the benzene ring maintained its GS symmetric form in the LE state, apart from a slight increase of all CC bonds,<sup>11</sup> exactly as in the case of the 1<sup>1</sup>B<sub>2u</sub> state of benzene.<sup>40</sup> The geometry of the donor or acceptor groups was almost unchanged compared to that of the ground state, and the dipole moment changed only slightly. All these features are typical for the transition to a covalent LE excited state in which the donor and the acceptor are spectators.

Table 3 reports for comparison the structures of the two stationary points on the ground surface of the corresponding anion radicals.

The calculated structures of the benzene moiety in the CT-(Q) states of all four molecules are very similar to each other

**Table 3.** Computed Optimized Geometries of the Two Lowest-Lying States of DMA, DMABN, PP, and PBN Anion Radicals (Bond Lengths in Å, Angles in deg); DMA: CASSCF(9/7)DZV; DMABN: CASSCF(13/10)cc-pVDZ; PP: CASSCF(13/10)DZV; PBN: CASSCF(13/11)DZV

anion radical	DMA	DMABN	PP	PBN
term	1 <sup>2</sup> B (Q)	1 <sup>2</sup> B (Q)	1 <sup>2</sup> B (Q)	1 <sup>2</sup> B (Q)
C1–C2	1.445	1.422	1.444	1.421
C2–C3	1.390	1.381	1.384	1.380
C3–C4	1.447	1.449	1.418	1.444
C1–N1	1.453	1.434	1.441	1.441
N1–C7	1.442	1.453	1.390	1.374
C4–C9		1.407	-	1.413
C9–N2		1.197	-	1.194
C7–C9			1.400	1.386
C9–C10			1.422	1.429
φ		90	11	48
term	1 <sup>2</sup> A (AQ)	1 <sup>2</sup> A (AQ)	1 <sup>2</sup> A (AQ)	1 <sup>2</sup> A (AQ)
C1–C2	1.415	1.408	1.405	1.396
C2–C3	1.461	1.458	1.460	1.453
C3–C4	1.405	1.398	1.396	1.396
C1–N1	1.432	1.434	1.450	1.444
N1–C7	1.449	1.449	1.378	1.385
C4–C9		1.456	-	1.456
C9–N2		1.181	-	1.181
C7–C9			1.388	1.384
C9–C10			1.437	1.438
φ		90	46	29

and also to the structure of the corresponding state of the anion radicals, in line with the proposed model. The same trend is found for the CT(AQ) forms. In the Q form the benzene ring is quinoidal, as expected, but there are other significant changes with respect to the GS. The C<sub>phenyl</sub>–N<sub>amino</sub> bond is lengthened as is also the cyano CN bond. In the pyrrole derivatives, the pyrrole group undergoes a drastic change: the central CC bond becomes a double bond, whereas the two side CC bonds are now single bonds. This is in line with the transfer of an electron from the butadiene part, rather than from the nitrogen atom N1. Similar changes are found for the AQ form, except that the benzene ring has an antiquinoidal structure and the cyano CN bond length does not change.

(36) Weersink, R. A.; Wallace, S. C.; Gordon, R. D. *J. Chem. Phys.* **1995**, *103*, 9530.

(37) Warren, J. A.; Bernstein, E. R.; Seeman, J. I. *J. Chem. Phys.* **1988**, *88*, 871.

(38) Belau, L.; Haas, Y.; Rettig, W. *Chem. Phys. Lett.* **2002**, *364*, 157.

(39) Okuyama, K.; Numata, Y.; Odawara, S.; Suzuka, I. *J. Chem. Phys.* **1998**, *109*, 7185.

(40) (a) Langseth, A.; Stoicheff, B. P. *Can. J. Phys.* **1956**, *34*, 350. (b) Callomon, J. H.; Dunn, T. M.; Mills, I. M. *Philos. Trans. R. Soc. London, Ser. A* **1966**, *259*, 499. (c) Haas, Y.; Zilberg, S. *J. Am. Chem. Soc.* **1995**, *117*, 5387.

## Energy level diagram, DMABN

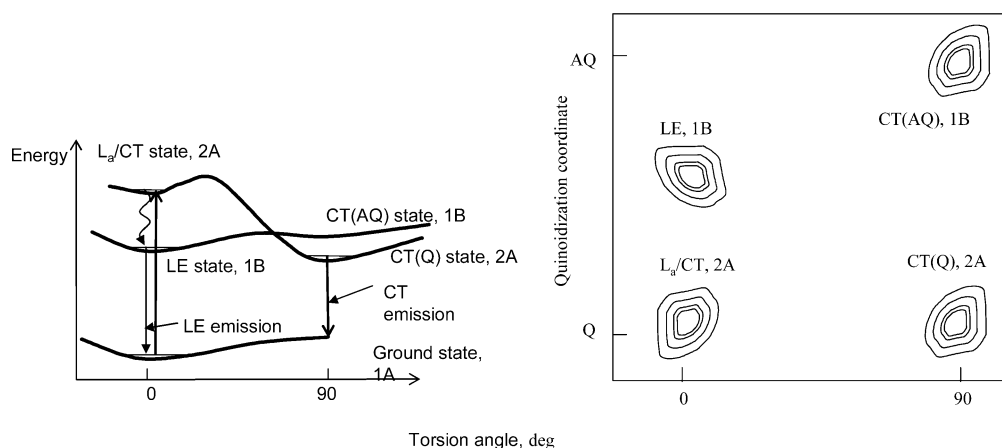


**Figure 5.** Schematic energy level diagram of DMABN (for numerical values, please see Table 1). The left panel shows the conventional presentation as a function of the torsion angle; straight lines represent radiative transitions, and the wavy line indicates a nonradiative process. The right-hand panel shows schematically the location of the different minima on the low-lying singlet excited states of DMABN along the quinoidization and the torsion coordinates.

**IV.c. Ionization Potentials.** Important parameters of the model are the ionization potential (IP) of the donor and the electron affinity (EA) of the acceptor. As it is well-known that the EA of benzene is negative (about  $-1.1$  eV),<sup>24,41</sup> energy must be supplied to the system for an electron to attach to the molecule. In terms of the diagram shown in Figure 2, the energy of  $D^{+\bullet} + A^{-\bullet}$  is thus *higher* than the energy of  $D^{+\bullet} + A + e^{-}$ . The experimental ionization potentials of trimethylamine and *n*-methylpyrrol (representing the donors) are 7.85 and 7.99 eV, respectively,<sup>42</sup> and the electron affinities of benzene and cyanobenzene are  $-1.11$  and  $-0.57$  eV, respectively.<sup>41</sup> The CASSCF calculation shows that the first ionization potential of the pyrrole derivatives is due to the extraction of an electron from the HOMO which is an a-type orbital centered on the butadiene fragment. The second IP is slightly higher ( $\sim 0.3$  eV) and is due to the ionization of the nitrogen lone pair orbital.

## V. Comparison with Experiment

**V.a. Absorption and Emission Spectra.** CASSCF calculations often over estimate the energies of the electronic excited states; this trend is evident from the data presented in Table 1. Since the main goal of this paper is to present the model, we defer efforts for more quantitative agreement with experiment to future work. The data presented in section IV, Table 1, thus serve as guidelines for the relative energies of the different states rather than as exact numerical estimates. In the case of DMA the LE state lies significantly lower than the CT states, accounting for the absence of dual fluorescence in this molecule.

A schematic energy level diagram for DMABN (as deduced from the model and the CASSCF calculations) is shown in Figure 5. The  $S_0$ – $S_1$  spectrum of DMABN<sup>43</sup> was measured at high resolution by fluorescence excitation. The authors concluded that the  $S_1$  state has a partial charge-transfer character. This is corroborated by the calculation: the lowest 1B state of the system has two minima, one at the geometry of the LE state, the other of the CT(AQ) state. The two, having the same sym-

metry, interact, leading to the partial CT character of the  $S_1$  state. The calculation also shows that the 2A state also has two minima, one can be assigned to the  $L_q/CT$  state, the other to the CT(Q) state, which in solution is the emitting CT state.

The calculated oscillator strength of the  $1A \rightarrow 2A$  transition ( $f = 0.43$ ) in the FC region is much larger than that of the  $1A \rightarrow 1B$  one ( $f = 0.078$ ). In solution, the stronger absorption band which is red-shifted with respect to the gas phase may completely mask the weaker one. Radiationless transitions lead to the population of the two emitting states, LE and CT(Q), the latter having a minimum at  $\theta = 90^\circ$ .

The spectra of PP and PBN were recently recorded in a supersonic jet. As noted in ref 38 the fluorescence excitation spectrum appears to be due to two close-lying states, but no assignment was offered. Okuyama et al.<sup>39</sup> analyzed the PP spectrum using a hindered rotor model which they assigned to the  $GS \rightarrow LE$  transition. In the more extended spectrum of Belau et al.,<sup>38</sup> a different series of bands appears at about  $800\text{ cm}^{-1}$  which was tentatively assigned to a different electronic state. In the excitation spectrum of PBN, a very pronounced change in the spectrum occurs at about  $400\text{ cm}^{-1}$  above the origin. The second transition is about 10 times as intense as the first. Following the present work, we tentatively propose that the first band observed for PBN in a supersonic jet is due to a  $GS \rightarrow LE$  transition and the second to a  $GS \rightarrow CT$  one. This assignment is supported by the high oscillator strength calculated for the 2A state at the FC region—about 0.38 (Table S1). This assignment is also compatible with the finding that PBN shows dual emission in an argon matrix and that the CT state can be directly excited in the matrix<sup>44</sup> even at lower energies than the LE(B) state: the matrix stabilizes the CT state more than the LE state due to the polarizability of argon and allows the observation of emission from both states, whereas in the gas phase only one of them fluoresces. The proposed structures of the minima on the excited electronic states are shown in an energy level diagram (analogous to that of Figure 5) given in the Supporting Information (Figure S1).

(41) Jordan, K. D.; Burrow, P. D. *Chem. Rev.* **1987**, *87*, 7. (b) Burrow, P. D.; Michejda, J. A.; Jordan, K. D. *J. Chem. Phys.* **1987**, *86*, 9.  
 (42) NIST Chemistry WebBook, NIST Standard Reference Database, 69, June 2005 release.  
 (43) Nikolaev, A. E.; Myszkiewicz, G.; Berden, G.; Meerts, W. L.; Pfanstiel, J. F.; Pratt, D. W. *J. Chem. Phys.* **2005**, *122*, 084309.

(44) Schweke, D.; Baumgarten, H.; Haas, Y.; Rettig, W.; Dick, B. *J. Phys. Chem. A.* **2005**, *109*, 576.



Zachariasse and co-workers found a good correlation between the tendency for dual emission and the energy gap between  $S_1$  and  $S_2$  as expressed in the absorption spectrum in solution.<sup>6</sup> The fact that DIABN is found to exhibit CT emission in the gas phase was attributed to the small energy gap.<sup>45</sup> Our model is in line with this observation, as the ionization potential of the alkylamines decreases as the alkyl group increases.

**V.b. Structure.** The experimental rotational constants of DMABN<sup>43</sup> are compared with our calculated ones in the Supporting Information (Table S2). Although the computed data for the three excited states appear to be similar, comparison with experiment indicates that the transition is to the LE state: the difference between the B and C rotational constants is larger in its case than that in the CT states, and fit better the data of ref 43. Several attempts were made to measure structural properties of the CT state. An X-ray study of DIABN was interpreted as showing that the CT state is planar;<sup>46</sup> changes in bond distances were not reported, perhaps as they were too small to measure. An indirect method for estimating bond-length changes is by comparing the vibrational frequencies in the CT state to those in the ground state—a decrease in a stretch vibration frequency is interpreted as indicating lengthening of the corresponding bond. Numerous efforts to measure the vibrational frequencies of DMABN and PBN in the CT state by picosecond IR<sup>47</sup> or resonance Raman spectroscopies<sup>48</sup> were made. The most significant changes were found to be a decrease in the frequency of the  $C_{\text{phenyl}}-N_{\text{amine}}$  stretch mode and the cyano CN stretch. These changes were considered as an indication that these bonds are weakened. The increase in the  $C_{\text{phenyl}}-N_{\text{amine}}$  bond is compatible with the TICT model, whereas an increase in the cyano CN bond fits better with the PICT one. Inspection of Table 3 shows that in both the CT(Q) and CT(AQ) forms, the  $C_{\text{phenyl}}-N_{\text{amine}}$  bond is lengthened. The cyano CN bond is longer in the Q form than in the ground state and remains unaffected in the AQ one. These results support the notion that the observed CT emission is due to the CT(Q) form. The measured cyano CN frequency is similar to that observed for the benzonitrile anion in solution,<sup>49</sup> lending further support to the model. The main difference between the two CT forms is in the structure of the phenyl moiety, which carries two double bonds between the central atoms (C2-C3 and C5-C6) in the Q-form and two nearly single bonds in the AQ form. If the corresponding vibrational stretching modes can be separated from other groups in the molecules, the stretch frequency is expected to be higher in the Q-form (about  $1600\text{ cm}^{-1}$ ) than in the AQ-form (around  $1400\text{ cm}^{-1}$ ). Current experimental values<sup>47,48</sup> appear to support the latter option.

## VI. Discussion

The possible role of a pseudo JT distortion in the photophysics of DMABN was alluded to by Schuddeboom et al.,<sup>6</sup> and

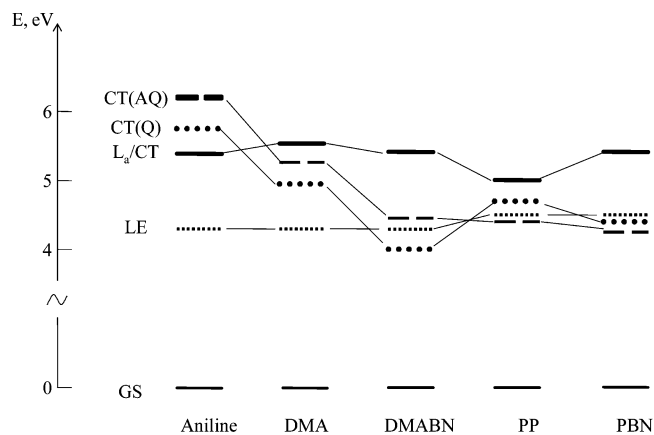


**Figure 6.** Ordering of the energy levels (at their minima) of aniline, DMA, DMABN, PP, and PBN, showing that aniline and DMA are not expected to exhibit DF, while the opposite is true of DMABN, PP, and PBN. The energy scale is given for rough orientation rather than exact data, based on experimental observations. The lower LE levels of PP and PBN are about 0.3 eV higher than those of the anilines. In the anilines, the lower-lying CT state is Q-type, whereas in the pyrrole derivatives it is the AQ-type.

Zachariasse et al.<sup>50</sup> However, as far as we know, this is the first attempt to connect the JT distortion of the benzene anion with the electronic nature of the CT states and the origin of dual fluorescence of DMABN and other benzene derivatives.

The role of quinoidal and anti-quinoidal forms of the molecules have been discussed by several authors<sup>11,14,17,51</sup> using various computation techniques. In our model the most important nuclear coordinate involved in the electron transfer is the quinoidization coordinate and not the twist angle. In comparing our computational results with previous ones it should be noted that this is the first large-scale CASSCF computation of DMABN that includes complete optimization of each excited state. A previous CASSCF calculation<sup>16</sup> used a much smaller active space (4e/4o or 6e/5o) compared to our much larger ones. Important early works<sup>52,53</sup> calculated only the energies of excited states reached upon vertical excitation and considered the effect of torsional angle change, but did not attempt to optimize the geometry of the excited states. In ref 11 a large active space (12/11) was used for the study of DMABN; the minima identified on the excited-state potential correlate well with ours: their  $S_1$  T(ICT) (the emitting CT state) corresponds to our Q(CT) state, and the LE states are likewise similar. The small differences in numerical values are due to the different basis sets used.

**VI.a. What Systems Are Expected To Exhibit DF in the Gas Phase? The Roles Played by the Acceptor and Donor Groups.** DF can only be observed if two separate minima exist on the first electronically excited surface of the molecule. The electrostatic model discussed in section II predicts that the energy of two CT states will be similar to the energy of the first excited LE state for donors having a small IP and acceptors having a large EA. Figure 6 shows schematically an overview of the expected energy level diagrams for aniline, DMA, DMABN, PP, and PBN.<sup>54</sup>

(45) Daum, R.; Druzhinin, S.; Ernst, D.; Rupp, L.; Schroeder, J.; Zachariasse, K. A. *Chem. Phys. Lett.* **2001**, *341*, 272.

(46) Techert, S.; Zachariasse, K. A. *J. Am. Chem. Soc.* **2004**, *126*, 5593.

(47) (a) Okamoto, H.; Inishi, H.; Nakamura, Y.; Kohtani, S.; Nakagaki, R. *J. Phys. Chem. A* **2001**, *105*, 4182. (b) Okamoto, H.; Kinoshita, M. *J. Phys. Chem. A* **2002**, *106*, 3485.

(48) (a) Ma, C.; Kwok, W. M.; Matousek, P.; Parker, A. W.; Phillips, D.; Toner, W. T.; Towrie, M. *J. Photochem. Photobiol. A* **2001**, *142*, 177. (b) Ma, C.; Kwok, W. M.; Matousek, P.; Parker, A. W.; Phillips, D.; Toner, W. T.; Towrie, M. *J. Phys. Chem. A* **2002**, *106*, 3294.

(49) Juchnovski, I.; Tsevatanov, Ch.; Panayotov, I. *Monatsh. Chem.* **1969**, *100*, 1980.

(50) Zachariasse, K. A.; von der Haar, T.; Hebecker, A.; Leinhos U.; Kühnle, W. *Pure Appl. Chem.* **1993**, *65*, 1745.

(51) Rappoport, D.; Furche, F. *J. Am. Chem. Soc.* **2004**, *126*, 1277.

(52) Serrano-Anders, L.; Merchan, M.; Roos, B. O.; Lindh, R. *J. Am. Chem. Soc.* **1995**, *117*, 3189.

(53) Parusel, A. B.; Köhler, G.; Nooijen, M. *J. Phys. Chem.* **1999**, *103*, 4056.

**VI.b. Comparison of Pyrrole and Aniline Derivatives.** CT emission appears to be more readily encountered in the pyrrole derivatives than the in corresponding aniline one. Thus, PP emits DF in acetonitrile, whereas DMA does not; PBN was found to display DF in clusters with acetonitrile in the gas phase and also in an argon matrix;<sup>44</sup> DMABN does not exhibit DF under these conditions. Moreover, PP was observed to emit CT fluorescence in an argon matrix doped by acetonitrile,<sup>55</sup> whereas no CT emission was observed from DMABN under similar conditions. This is in apparent contradiction with the proposed model, as trimethylamine has a lower IP than *N*-methylpyrrol. Indeed, the experimental dipole moment of the CT state of DMABN is larger than that of PBN.

A possible explanation for this apparent deviation from the model is the higher energy of the LE state in the pyrrole derivatives—in the case of PP it is higher than that of DMA by about 0.3 eV (Table 3, experimental data), compensating for the higher ionization potential. A similar situation holds for the DMABN/PBN pair.

Another difference between the two families is the nature of the low-lying CT state. In the pyrrole derivatives the model predicts a practically free internal rotation around the C<sub>phenyl</sub>–N<sub>amino</sub> bond. The experimental observation of CT emission from PBN in argon matrixes<sup>44</sup> is thus not a surprise—there is no need for large amplitude motion in this molecule for DF to occur. The same argument explains the dual emission of PP observed in acetonitrile-doped argon matrixes.<sup>55</sup> As the role of torsion around this bond was the subject of much discussion, the next subsection summarizes the predictions of the model concerning this issue.

**VI.c. Role of Torsion around the C<sub>phen</sub>–N<sub>amino</sub> Bond: TICT or PICT.** As can be surmised from the MO picture, in the CT(AQ) form, the benzene  $\pi$  MO has a node at C1. The C<sub>phenyl</sub>–N<sub>amino</sub> bond is essentially a single bond for any torsional angle. For the CT(Q) form, there is a difference between the aniline and pyrrole derivatives. As the donor orbital of the pyrrols has a node at N1, there is no contribution to the bonding in the C<sub>phenyl</sub>–N<sub>amino</sub> bond. In the aniline derivatives, the  $\pi$  electrons of the nitrogen atom can interact with the benzene  $\pi$  system, creating partial double bond character in the planar geometry. Under these conditions, charge transfer is less efficient (section II), and the dipole moment of the planar form is smaller than that of the perpendicular form, in which the two  $\pi$  systems are decoupled. In that sense the perpendicular Q and AQ forms are true TICT cases—a complete charge transfer is possible.

Inspection of Table 2 shows that in both states the C<sub>phenyl</sub>–N<sub>amino</sub> bond is considerably longer than that in the ground state. For both quinoid and anti-quinoid structures, rotation around the C<sub>phenyl</sub>–N bond is therefore quite facile. It is concluded that for the pyrrole derivatives the TICT and PICT models are not really mutually exclusive—the system may in principle emit CT-type fluorescence from either a planar or perpendicular conformation (or any torsion angle). Thus, CT emission from the planarized pyrrole derivative<sup>8</sup> is readily accounted for.

For DMABN and other aniline derivatives the L<sub>a</sub>/CT state in the planar form is connected via a barrier with the

perpendicular CT(Q) form, which has a larger dipole moment. CT emission of DMABN is thus from the twisted form.

The temperature dependence of the CT emission has been the focus of much experimental and theoretical work. The TICT model attracted most attention, as the large amplitude motion it entails is expected to be restricted by friction, as argued in many papers.<sup>12,56–59</sup> According to our model, the crucial change is the rearrangement of the  $\pi$  electrons to form the Q or AQ states. In terms of solvent cage, these changes are minor and not expected to be met with the frictional resistance of the medium. Yet, the fact that the CT(Q) state is optimized in the perpendicular form turns out to have important kinetic consequences and to be the dynamically most significant feature of the process. The small observed thermal barriers are probably due to the existence of a conical intersection nearby.<sup>11,14</sup> The thermal route between two minima around the degeneracy is characterized by a shallow potential well. The system has to surmount a rather small energy barrier as it moves in a trajectory resembling a “Mexican Hat”. This unique situation could be the reason for the difficulty in interpreting the temperature dependence.

**VI.d. Comparison with the Previous Model (ref 14).** In a previous paper from this group<sup>14</sup> the Q and AQ states were introduced, and their role as possible CT states was discussed. It was assumed that the Q form is planar, and its optimization was carried out only for this geometry. Since the model proposed in this paper is an extension of the previous one, it is appropriate to discuss and explain the differences between the two models.

The main difference lies in the physical nature of the model. The former one (ref 14) was based on the properties of the excited states of the neutral benzene molecule, whereas the present model is based on the properties of the benzene anion radical. Since the excited state potential surface of the molecules is very complex, a search of possible structures must be guided by a theoretical model. In the case of the previous model it was assumed that the basic features of the model may be found by considering only C<sub>2v</sub> structures; furthermore, considering the B<sub>2u</sub> and B<sub>1u</sub> excited states of benzene as the basis of the model, only the planar Q-form (which corresponds to the L<sub>a</sub>/CT state of the present paper) was investigated. The introduction of the Jahn–Teller distorted forms of the benzene anion radical as the basis of the model necessitated considering all possible geometries for both the CT(Q) and CT(AQ) forms (i.e. C<sub>2</sub> symmetry rather than C<sub>2v</sub> symmetry). This is most easily understood by considering the frontier MOs as discussed in section II.

A further change made in this paper is the explicit comparison of aniline derivatives and pyrrole ones. As shown, the donor group is mainly the nitrogen lone pair for aniline derivatives and the butadiene part of the pyrrole derivatives. However, the HOMO-1 of PP and PBN, which is mainly the nitrogen lone pair one, is energetically quite close, and transitions from this orbital will lead to states analogous to those of the anilines.<sup>60</sup> A calculation of the states arising from this excitation shows

(54) In this figure, as in the subsequent discussion, the structures shown were found computationally to be stationary points (minimax). These structures are expected to persist as stationary points in a liquid solvent environment, wherein the more polar structures become minima.

(55) Schweke, D.; Haas, Y. *J. Phys. Chem. A* **2003**, *107*, 9554.

(56) Huppert, D.; Rand, S. D.; Rentzepis, P. M.; Barbara, P. F.; Struve, W. S.; Grabowski, Z. R. *J. Chem. Phys.* **1981**, *75*, 5714.

(57) Hicks, J. M.; Vandarsall, M. T.; Sitzmann, E. V.; Eisenthal, K. B. *Chem. Phys. Lett.* **1987**, *135*, 413.

(58) Kajimoto, O.; Nayuki, T.; Kobayashi, T. *Chem. Phys. Lett.* **1993**, *209*, 357.

(59) Saielli, G.; Polimeno, A.; Nordio, P. L.; Bartolini, P.; Ricci, M.; Righini, R. *Chem. Phys.* **1997**, *223*, 51.

(60) We thank a reviewer for pointing this out.

that they are of A symmetry ( $A_2$  in  $C_{2v}$ ) and higher lying than the states derived from the butadiene orbital. For both PP and PBN the energies of the second CT states (both Q' and AQ') are higher than those of the corresponding first CT state by about 0.5 eV, a value similar to the difference between the HOMO (butadiene-centered) and HOMO-1 (lone pair).

## VII. Summary

A model accounting for the dual fluorescence of aniline and phenylpyrrol derivatives is presented. The emitting charge transfer state is due to the transfer of an electron from the donor group to the benzene ring, creating a derivative of the benzene anion radical. Two electronic states are necessarily formed as a consequence of the Jahn–Teller distortion of the benzene anion radical: one has a quinoid structure, the other, an antiquinoid one. The energy balance determined by the ionization potential of the amino groups, the electron affinity of benzene or benzonitrile, and the distance between donor and acceptor makes the CT state(s) almost iso-energetic with the LE state in the aniline and phenylpyrrol derivatives. Use of  $C_2$  symmetry clearly underscores the correlation between different minima on the two lowest-lying electronic states of 1B and 2A symmetry. Both are found to support at least two local minima

In the aniline derivatives, the donor orbital is mainly the lone pair of the amino nitrogen atom, whereas in the pyrrole derivatives, the major contribution is from the butadiene part of the pyrrole fragment. In the CT(AQ)-form, torsion around the  $C_{\text{phenyl}}-N_{\text{amino}}$  bond is quite facile for both pyrrole and aniline derivatives. The system tends to twist away from the planar configuration in a polar solvent as its dipole moment is smaller in the planar geometry than in the twisted one. This explains the origin of the TICT model. In the gas phase, different angles were computed for PBN in the CT forms. The observation of CT emission of PBN in an argon matrix, where torsion is presumably prohibited, is thus explained by the model. For the aniline derivatives the planar Q-form has a local minimum

at the La/CT state but the global minimum is at the perpendicular geometry.

In the model, the role of the CN group is essentially restricted to enhancing the electron-withdrawing power of the benzene ring. Therefore, its position relative to the donor is not crucial, and meta-substituted PBN should exhibit CT emission, as observed experimentally.<sup>13</sup> The absence of dual emission in meta-DMABN is explained by the large energy gap between the CT and LE state—the LE state is lower in energy as expected from the meta effect.<sup>61</sup>

Finally, the model provides a simple explanation for the direct excitation of the CT states (i.e. not via the LE state) observed in supersonic jets and in argon matrixes. The optical transition connecting the ground state with the emitting CT state is often not observed, particularly in liquid solutions and normal temperatures, as it is much weaker than the neighboring  $S_0-S_2$  transition in the Franck–Condon region.

**Acknowledgment.** This research was supported by the Israel Science Foundation and by The Volkswagen-Stiftung (I/76 283). The Farkas Center for Light Induced Processes is supported by the Minerva Gesellschaft mbH.

**Supporting Information Available:** Table S1 lists the experimental and calculated rotational constants of DMABN in the low-lying singlet states; Table S2 lists the experimental and calculated rotational constants of DMABN in the low-lying singlet states; Table S3 lists the geometries (as Cartesian coordinates) for all of calculated structures; Figure S1 shows schematically the location of the different minima on the low-lying singlet excited states of PBN along the quinoidization and the torsion coordinates; and complete refs 33 and 34. This material is available free of charge via the Internet at <http://pubs.acs.org>.

JA0548945

(61) Grinter, R.; Heilbronner, E.; Godfrey, M.; Murrell, J. N. *Tetrahedron Lett.* **1961**, *21*, 771.